similar under these conditions, the method gives a rough measure of the photons absorbed by sensitizer during continuous photolysis.

Individual determinations were generally repeated four times. External methyl viologen was measured immediately before and after illumination using freshly prepared dithionite solution. In instances where the viologen radical cation had accumulated as a consequence of photolysis, it was reoxidized by pulsing the solution with O_2, then repurging of residual oxygen before dithionite addition.

Instrumentation. Optical measurements were made on a Cary 16 spectrophotometer. Pulsed laser experiments of type II MV^{2+}/DHP/$ZnTMPyP^{4+}$ vesicles were made in Michael Grätzel's laboratory at EPFL, Lausanne, Switzerland, using as excitation source a 20-ns pulse (532 nm) from a frequency doubled Nd:YAG laser. Light scattering measurements were also made at EPFL using a Chromatix KMX-6 photometer interfaced to a Langley-Ford autocorrelator.

Experiments in Potsdam. Preparation of Type II Asymmetrical MV^{2+}/DHP/$Ru(bpy)_3^{2+}$ Vesicles. A sample containing 10.5 mg of DHP (Sigma) was heated in 4.0 mL of 0.01 N Tris-HCl buffer at pH 7.6 for 5 min at 80 °C prior to sonicating for 5 min at the same temperature using the microtip of a Braunsonic sonifier set at 70 W. Methyl viologen (Aldrich, twice recrystallized from cold methanol) solution (4.6 mg in 2.0 mL of 0.01 N Tris-HCl buffer, pH 7.6) was added slowly with repeated sonication (at 70 W) to the DHP vesicles, kept at 80 °C. Total additional sonication time was 25 min. Subsequent to cooling to room temperature (in the dark) the vesicle solution was centrifuged for 20 min in a table-top centrifuge. The supernatant was passed through a prewashed and equilibrated (0.01 N Tris-HCl, pH 7.6) Sephadex G 50-80 column (21.7 × 0.7 cm) using 0.01 N Tris-HCl, pH 7.6 as the eluant; 3.5-mL fractions were collected in a fraction collector. Quantitative examination of the elution fraction profile established 99.9% recovery of MV^{2+} of which 1.8% appeared in the vesicle fraction. The vesicle fractions (fractions 5 and 6) were passed twice through a prewashed and equilibrated (with 0.01 N Tris-HCl buffer, pH 7.6) Chelex 100 (Biorad 200-400 mesh, sodium form). The vesicle fraction contained less than 1% methyl viologen outside, as determined by the $Na_2S_2O_4$ test.[2]

MV^{2+} Determinations. $Na_2S_2O_4$ stock solutions were made freshly in 0.1 N Tris-HCl buffer at pH 7.6. In typical measurements 50 μL of 4.0 × 10^{-2} M $Na_2S_2O_4$ stock solution was added to 1.0 mL of deoxygenated (purified argon bubbled) vesicle solution. Concentration of the MV^+ was determined spectrophotometrically using a Cary 118C spectrophotometer.[2] Two sets of experiments were carried out to determine MV^{2+} leakage. In the first set of experiments $Na_2S_2O_4$-induced leakage was determined in MV^{2+}/DHP vesicles. In the second set of experiments effects of photosensitized MV^{2+} leakages were determined. Irradiations were carried out in a cell thermostatted at 26 °C. The IR band of the light was removed by passage through distilled water. Five separate measurements were carried out for each set of experiments. Mean rates of MV^{2+} leakages, $\Delta Abs/\Delta t$ values, were determined to be 3 × 10^{-5} s^{-1} and 4.8 × 10^{-5} s^{-1} in the absence and in the presence of irradiation, respectively. These correspond to 2% and 3.2% MV^{2+} leakage per 5 mi. Estimated error in these measurements is 30%. Laser flash photolysis and steady-state fluorescence quenching experiments have been previously described.[2]

Acknowledgment. Support of this work by the U.S. Public Health Service (GM-20943 to J.K.H.) and by the U.S. Department of Energy (to J.H.F.) is gratefully acknowledged. J.K.H. and L.Y-C.L. are grateful to Professor Michael Grätzel, Institut de Chimie Physique, EPFL, Lausanne, for use of his facilities and for his warm hospitality during the time these experiments were made. M.P. thanks CNPQ (Brazil) for fellowship support.

Registry No. $Ru(bpy)_3^{2+}$, 15158-62-0; $ZnTMPyP^{4+}$, 40603-58-5; methyl viologen dichloride, 1910-42-5; DHP, 84065-97-4.

A Classical Dynamics Model of Plasma Desorption Mass Spectrometry Experiments

Barbara J. Garrison†

Contribution from the Department of Chemistry, The Pennsylvania State University, University Park, Pennsylvania 16802. *Received May 10, 1982*

Abstract: A classical dynamics procedure is developed to model the desorption of particles from a surface due to heavy particle bombardment. The theoretical approach is to utilize a metallic (Ni) microcrystallite with up to 8 atomic layers covered with an organic monolayer such as benzene. This ensemble of atoms is then bombarded from both the front and the back of the microcrystallite to test whether there are fundamental differences in mechanisms by which the organic molecule is ejected between the two configurations. The model calculation is performed in order to evaluate the importance of collision cascades in the desorption of large molecules using plasma desorption mass spectrometry (PDMS) where a ~100-MeV incident particle bombards a thin foil from behind. This geometry contrasts that utilized in SIMS or FAB mass spectrometry experiments where the molecular layer is bombarded directly by a 1-5-keV heavy particle. The calculated results show that most of the predicted observables for the ejected benzene molecules, including their mass spectrum and their energy and polar angle distributions, are similar. The energy distributions of the benzene molecules are Maxwell-Boltzmann-like in character even though the desorption is a consequence of a nonequilibrium energetic collision cascade. The details of the collision events that lead to desorption of particles, however, are quite different between the two calculations. These collisional differences are most apparent in the angular distributions of the ejected Ni atoms. They also indicate that molecular ejection is slightly more favorable when bombarding from behind the microcrystallite than when bombarding the sample directly, since the direction of momentum need not be reversed.

Mass spectral studies have recently become routine for experimental investigation of molecules with masses in the 1000-20000-amu range. In particular, two techniques that employ energetic beams of heavy particles to produce the molecular ion are currently being developed with considerable success. With one approach the sample is bombarded with a beam of atoms (or ions) and the ionic species that desorb from the surface are then detected with a mass spectrometer. The distinctive feature in this experiment is that the beam source and the detector are on the same side of the sample (Figure 1). This technique is called secondary ion mass spectrometry (SIMS)[1] if an ion beam is employed or fast atom bombardment mass spectrometry

† Alfred P. Sloan Research Fellow.

(1) B. J. Garrison and N. Winograd, *Science*, **216**, 805 (1982).

0002-7863/83/1505-0373$01.50/0

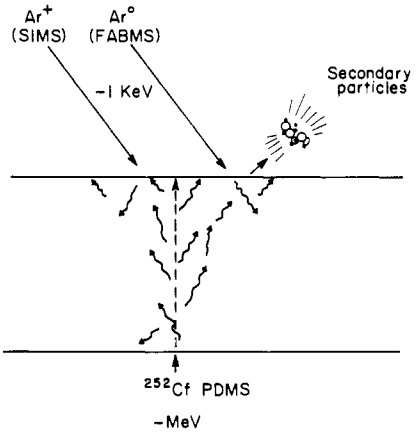

Figure 1. Schematic of the energetic collision cascade processes.

(FABMS)[2] if an atom beam is used. Typically the particles in the incident beam have hundreds or thousands of electron volts of kinetic energy. Alternatively the sample can be bombarded from the backside by a particle with approximately 100 MeV of kinetic energy. A clever approach to obtain these energetic particles is to employ a fission product from a decaying ^{252}Cf nucleus,[3] although particles from accelerators are also used as the probe.[4] This technique is often called plasma desorption mass spectrometery (PDMS). The two approaches appear, at least from the experimental setup, to be quite different, yet the spectra produced by each are similar.[5]

The desorption of atoms and molecules in the SIMS and FABMS experiments is generally believe to occur because the kinetic energy of the incident particle is converted into kinetic energy of the atoms in the sample.[1] The species that have sufficient momentum toward the vacuum above the solid then desorb. This process occurs in less than 200–300 fs (10^{-15} s). The short duration of this process apparently allows molecules that would decompose if heated to be volatilized without degradation. The exact mechanism or mechanisms of the energy conversion process in the PDMS experiments, however, are still open to discussion. There is evidence for electron-hole pair formation due to the passage of the energetic particle through insulator samples.[5] Regardless of the initial energy conversion process, however, we feel that in the final femtoseconds in both experiments an energetic collision cascade is set up in the solid causing particles to desorb from the surface. This belief results in part from a similarity of the spectra produced by each technique. The parent ion (+/− one proton or as a cationized species) is often the most intense peak.[1,3-8] The spectra can exhibit fragmentation patterns that are characteristic of the species and the matrix, yet are not hopelessly complex. In addition, the energy distributions of the desorbed particles from both types of experiments are similar, with peaks at 1–3 eV.[5,9,10] The PDMS energy distributions tend, however, to lack a high-energy tail.[5,10]

A classical dynamics procedure has been used extensively to examine the fundamental processes and to predict observables from the SIMS or FABMS experiments.[1,9,11-20] This model follows in detail the nuclear motion in the solid that gives rise to the desorption of particles from the surface. From the final positions and momenta of the ejected particles, average number of particles ejected, energy distributions, angular distributions, and cluster formation probabilities can be predicted. In this study we use this same model to examine the important processes for ejection of particles if the collision cascade is initiated from the backside of a crystal. For this case, a crystallite with up to 8 atomic layers is bombarded by a 1-keV Ar particle. The goal is to examine the similarities and differences between collision cascades if the bombarding particle originates from the same side of the sample as the detector or the bombarding particle strikes from the backside (Figure 1). By comparing the predicted observables with those obtained from PDMS experiments it should be possible to evaluate the importance of the collision cascade process in the desorption of molecular species.

Due to the neglect of electronic processes, the calculations do not include variations in yield due to ionization of the ejected species at the surface. Thus, it is not possible to directly compare the calculated results to SIMS, FABMS, or PDMS experiments, although relationships have been found between the observables of the calculated neutral and measured ionic species.[1,16,18] In the remainder of this work, then, the terminology SIMS simulation or the PDMS simulation will be used simply to designate the original direction of the Ar primary particle.

In order to make direct comparisons between the results of this PDMS calculation and those from the backscattering or SIMS process two systems that have previously been theoretically examined in the SIMS mode have been chosen. The first is a series of Ni(001) crystallites of varying thickness up to 8 atomic layers. The second is a Ni(001) crystallite with an adsorbed $c(4 \times 4)$ overlayer of benzene molecules. In both simulations the bombarding particle is Ar with 1 keV of kinetic energy at normal incidence.

The most striking difference between the mechanisms of the two types of calculations arises simply from conservation of linear momentum. In the PDMS case, the initial momentum is in the same direction that the desorbed particles must move if they are to reach the detector. This forward scattering is much more efficient than backscattering which occurs in the case of the SIMS experiment, where the initial particle has momentum in the opposite direction of the final desorbed particles. In this latter case the momentum must be turned around before the atoms and molecules are struck in such a manner so that they will desorb. Mechanisms such as focussed collision sequences along close packed rows and channeling by open directions that were once thought to be important in sputtering or SIMS experiments[21] are much more important for desorption in the forward scattering or PDMS situation. Most notably this gives rise to very different azimuthal angle distributions of the ejected Ni atoms. Even though the details of the collision mechanisms are different, the predicted mass spectrum, energy distribution, and polar angle distribution of the ejected benzene molecules from the PDMS simulation are very similar to those from the SIMS simulation.

(2) M. Barber, R. S. Bordoli, R. D. Sedgewick, and A. N. Tyler, *J. Chem. Soc. Chem. Commun.*, 325 (1981).
(3) R. D. Macfarlane and D. F. Torgerson, *Science*, **191**, 920 (1976); R. D. Macfarlane, *Biomed. Mass Spectrom.*, **8**, 449 (1981).
(4) P. Dück, W. Treu, W. Galster, H. Fröhlich, and H. Voll, *Nucl. Instrum. Methods*, **168**, 601 (1980); P. Dück, H. Fröhlich, W. Treu, and H. Voit, *ibid.*, **191**, 245 (1981).
(5) R. D. Macfarlane, *Acc. Chem. Res.*, **15**, 268 (1982).
(6) A. Benninghoven, D. Jaspers, and W. Sichtermann, *Appl. Phys.*, **11**, 35 (1976).
(7) H. Grade, N. Winograd, and R. G. Cooks, *J. Am. Chem. Soc.*, **99**, 7725 (1977).
(8) C. J. McNeal and R. D. Macfarlane, *J. Am. Chem. Soc.*, **103**, 1609 (1981).
(9) R. A. Gibbs, S. P. Holland, K. E. Foley, B. J. Garrison, and N. Winograd, *J. Chem. Phys.*, **76**, 684 (1982).
(10) N. Fürstenau, W. Knippelberg, F. R. Krueger, G. Weiß, and K. Wien, *Z. Naturforsch. A*, **32A**, 711 (1977).
(11) B. J. Garrison, N. Winograd, and D. E. Harrison, Jr., *J. Chem. Phys.*, **69**, 1440 (1978).
(12) N. Winograd, D. E. Harrison, Jr., and B. J. Garrison, *Surf. Sci.*, **78**, 467 (1978).
(13) B. J. Garrison, N. Wingrad, and D. E. Harrison, Jr., *Phys. Rev. B: Condens. Matter*, **18**, 6000 (1978).
(14) B. J. Garrison, N. Winograd, and D. E. Harrison, Jr., *J. Vac. Sci. Technol.*, **16**, 789 (1979).
(15) D. E. Harrison, Jr., P. W. Kelly, B. J. Garrison, and N. Winograd, *Surf. Sci.*, **76**, 311 (1978).
(16) N. Winograd, B. J. Garrison, T. Fleisch, W. N. Delgass, and D. E. Harrison, Jr., *J. Vac. Sci. Technol.*, **16**, 629 (1979).
(17) N. Winograd, B. J. Garrison, and D. E. Harrison, Jr., *J. Chem. Phys.*, **73**, 3473 (1980).
(18) B. J. Garrison, *J. Am. Chem. Soc.*, **104**, 6211 (1982).
(19) R. P. Webb and D. E. Harrison, Jr., *Appl. Phys. Lett.*, **39**, 311 (1981).
(20) D. E. Harrison, Jr., *J. Appl. Phys.*, **52**, 1499 (1981).
(21) M. W. Thompson, in "Interaction of Radiation with Solids", R. Strumane et al., Eds., North-Holland, Amsterdam, 1964, pp 84–113.

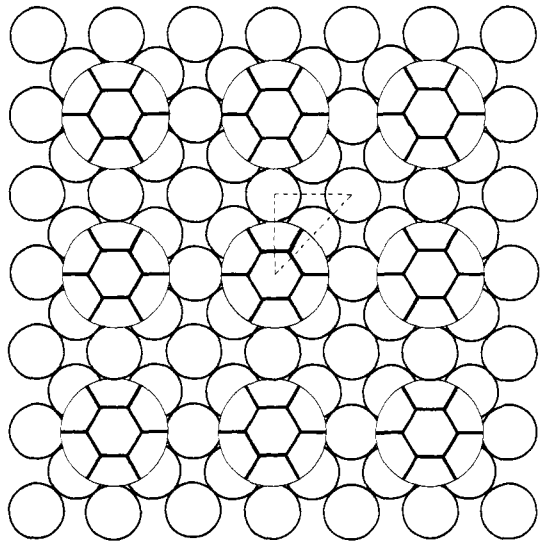

Figure 2. Placement of atoms. Ni(001) with a $c(4 \times 4)$ overlayer of benzene, C_6H_6. The dashed triangle is the impact zone for normal incidence bombardment. The circle around each benzene is the radial extent of the hydrogen position, 2.5 Å. The positions of the third-, fifth-, and seventh-layer Ni atoms are directly below those of the first-layer atoms. The atoms in the even-numbered layers are below the fourfold holes of the first layer.

As in the SIMS simulation we find the internal energy of the ejected benzene molecules to be such that most of the molecules will reach the detector without fragmentation.

Description of the Calculation

The clean nickel and nickel–benzene systems are modeled by a classical dynamics procedure developed over the past few years to study in detail the bombardment process and subsequent ejection of particles.[19,11-20] Briefly the theoretical model consists of approximating the solid by a finite microcrystallite. Assuming a pairwise interaction potential among all the atoms, Hamilton's equations of motion are integrated to yield the positions and momenta of all particles—the primary Ar atom or ion, the substrate Ni atoms, and adsorbate atoms in the benzene molecule—as a function of time during the collision cascade. The final positions and momenta can be used to determine such observables as total yield of ejected particles, energy distributions, angular distributions, and possible cluster formation.

In the clean nickel calculations the (001) crystal face is exposed to the detector. The calculations are performed on a series of crystallites of thickness varying up to 8 atomic layers. For the crystallites with 1–5 layers a surface size as shown in Figure 2 is used. For the crystallites with 6–8 layers two additional rows of atoms in each direction are included. In all cases the Ar particle has 1 keV of energy and bombards perpendicular to the backside of the crystal. A total of 110 Ar impacts are calculated for each crystal thickness. Due to uncertainties in the Ar–Ni interaction potential two different functional forms have been used, a Born–Mayer and a Moliere, for this interaction. The Moliere potential corresponds to smaller atom sizes at collision energies of interest than the Born–Mayer potential. Both potentials are given in ref 18.

The configuration of benzene molecules on the Ni(001) surface is shown in Figure 2 and described in detail in ref 18. The nickel substrate consists of 5 atomic layers. Again the Ar particle has 1 keV of energy and bombards perpendicular to the crystal. Only the Moliere potential is used for the Ar–Ni interactions. A total of 820 Ar impacts are calculated in order to obtain sufficient ejected molecules for statistically reliable energy and angular distributions. A corresponding SIMS simulation has previously been reported.[18]

Results and Discussion

The results from the calculations indicate that different mechanisms are important for the desorption of particles in the forward scattering or PDMS simulation than in the backscattering or SIMS simulation. Shown in Figure 3 are the yields of Ni atoms and Ni_2 clusters ejected per incident Ar particle vs. the number of atomic layers in the model microcrystallite in the PDMS calculation. The SIMS calculations were performed on a four-layer crystallite[9] and the resulting yields are also shown in Figure 3. For the same number of layers (four) the SIMS calculation predicts smaller yields than the PDMS simulation. If this experiment of bombarding a 4 atomic layer crystal from the backside could actually be performed, more efficient desorption processes should be expected. However, whereas the yields from the SIMS calculation are constant as the number of atomic layers increases,[12,22] as seen in Figure 3, the Ni atom yield in the PDMS calculation changes as the depth of the crystallite is varied. The critical parameter in comparing the efficiency of desorbing particles in the two calculations is the energy deposited per layer. For 1–3 atomic layers, many of the Ar particles pass through the sample retaining a considerable portion of their original energy. As the number of layers increases most of the Ar energy is deposited into the crystal. This 1 keV of Ar kinetic energy must be shared among all the layers so as the number of layers increases further the energy near the surface must decrease, and the yield decreases. In contrast, the top layer is nearest the beam origin in SIMS and the yields are relatively independent of whether 4 or 100 layers are used in the calculation. It is interesting to note that while the potential form of the Ar–Ni interaction can affect

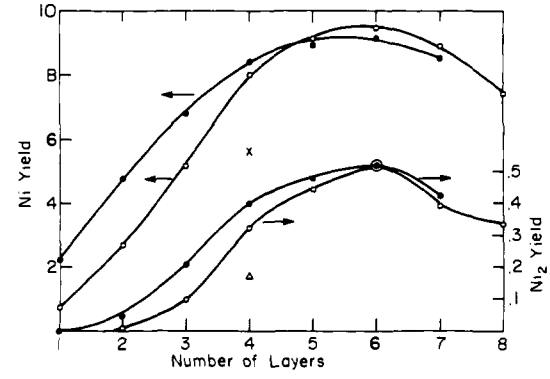

Figure 3. Ni and Ni_2 yield from clean Ni(001) vs. number of layers in the crystal. For the calculations with 1–5 layers the surface crystal size is shown in Figure 2. For the calculations with 6–8 layers two additional rows in each direction are included. (●) Born–Mayer potential for the Ar–Ni interaction (PDMS simulation); (○) Moliere potential for the Ar–Ni interaction (PDMS simulation); (×) value of the Ni yield from a SIMS calculation when a Born–Mayer potential is used; (△) value of the Ni_2 yield from a SIMS calculation when a Born–Mayer potential is uded.

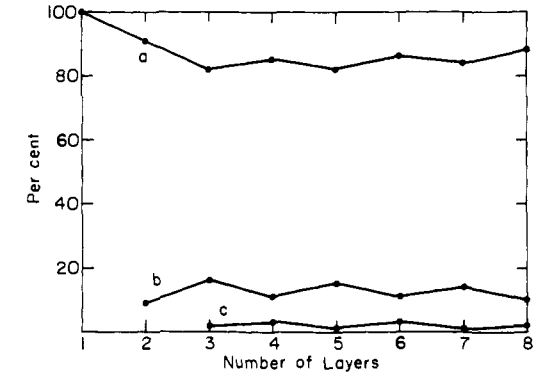

Figure 4. Percentage of the total Ni yield from each layer vs. number of layers from the PDMS simulation. The Moliere potential is used for the Ar–Ni interaction. (a) First-layer contribution; (b) second-layer contribution; (c) third-layer contribution.

(22) The crystal size is chosen so that a further increase in the number of atoms does not alter the predicted yield.

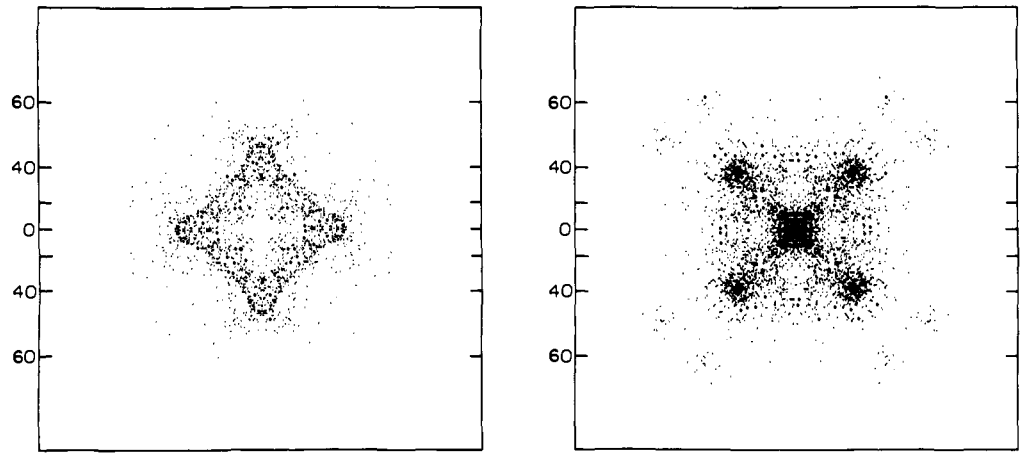

Figure 5. Angular distributions of the ejected Ni atoms. See text for description. The numbers on the ordinate refer to the polar deflection angle given in degrees. The plate is oriented the same as the crystal in Figure 2. The left panel is from the SIMS simulation and shows only those Ni atoms with greater than 20 eV of kinetic energy. The right panel displays all Ni atoms with greater than 100 eV that eject in the PDMS simulation.

the calculated SIMS yields by as much as 100%[18] there is virtually no effect of the potential on the predicted yields from the PDMS simulation (Figure 3).

This more efficient forward scattering causes a significant number of particles to desorb from beneath the first atomic layer. In the SIMS calculation 96% of the ejected Ni atoms were originally in the first layer, 4% in the second layer, and less than 0.1% in the third layer. As seen in Figure 4, there is a considerable contribution (15–20%) to the PDMS yield from layers 2 and 3. There are also a few atoms that eject from the fourth and fifth layers. More of the Ni_2 dimers contain second-layer atoms in the PDMS simulation than in the SIMS case. In the SIMS C_6H_6/Ni(001) calculations ~10% of the Ni_2 dimers contain a second-layer atom. In the PDMS C_6H_6/Ni(001) calculation this percentage more than doubles. Often the dimer is formed by a second-layer atom moving through the fourfold hole in the surface by combining with one of the first-layer atoms surrounding the hole. This mechanism has been proposed for dimer formation in SIMS experiments[23] although we have not found it to dominate in any of our previous calculations. As seen from this study, forward scattering is necessary for this cluster formation mechanism to have a high probability.

The angular distributions of ejected atoms have been shown to reflect their local geometry in the original surface.[9,24-28] This is especially valid for the high-energy particles that eject early in the collision cascade before the surface has been damaged. Shown in Figure 5 is the angular distribution of Ni atoms with kinetic energy greater than 20 eV ejected in the SIMS calculation with the overlayer of benzene molecules. This data set is used because more Ar impacts were calculated resulting in smaller statistical fluctuations. The qualitative results are the same for the clean metal calculations. Each ejected atom is plotted on a flat-plate collector an arbitrary distance above the crystal. The radial distance of a plotted point from the center of the plate is proportional to the polar angle of ejection of the atom. The orientation of the plate is the same as in Figure 2. The high-energy Ni atoms tend to eject in the ⟨100⟩ directions (horizontal and vertical), channeled through the fourfold holes. The angular distribution of Ni atoms ejected in the PDMS calculation with the benzene molecule overlayer is also shown in Figure 5. Here

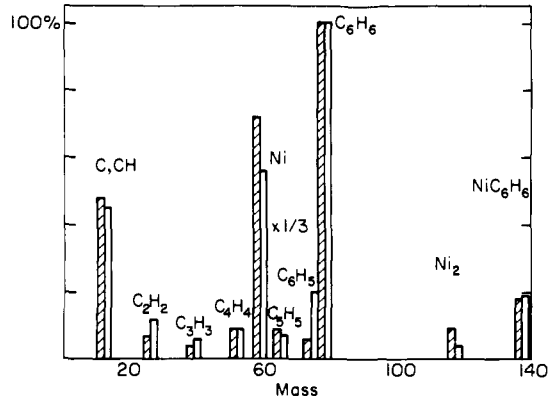

Figure 6. Calculated benzene mass spectra. The open histograms refer to the SIMS simulation and the shaded ones to the PDMS simulation.

only the Ni atoms with greater than 100 eV of kinetic energy are plotted. There are virtually *no* Ni atoms in the SIMS calculation with this much energy. The PDMS angular distribution is almost orthogonal to the SIMS one. Of the atoms contributing to the PDMS distribution in Figure 5, over 60% of them originated from below the first layer. The central region of high intensity arises mainly from second- and fourth-layer atoms that were directly above the incident Ar particle. The Ni atoms are channeled straight up through the fourfold hole by nearly head-on collisions. There are also regions of high intensity rotated 45° from the horizontal and vertical directions. These are also due in a large part to second-layer atoms that are struck by glancing collisions and thus eject through a neighboring fourfold hole. These mechanisms are very different from those operative for ejection of highly energetic particles in the SIMS process.

Although the ejection yields of benzene molecules and fragments are higher in the PDMS simulation than in the SIMS simulation, the mass spectra are virtually identical (Figure 6). The C_6H_6 yield from the SIMS calculation is 1.2 molecules per incident ion vs. 2.6 molecules per ion in the PDMS case. The intensities in Figure 6 are normalized to the C_6H_6 peak with only those species that are at least 5% of the C_6H_6 peak shown. The hydrocarbon fragments are predominantly characterized by equal numbers of carbon and hydrogen atoms with the parent species being by far the most intense. Due to the interaction potentials used, the number of carbon atoms in a fragment must always be greater than or equal to the number of hydrogen atoms. These spectra have not been corrected for the probability of the species becoming ions during ejection, the stability of a fragment (e.g., C_5H_5 is not stable), or the possible further fragmentation of larger species on the way to the detector. Besides the species indicated in the spectrum, the calculations predict clusters of the types C_nH_m, NiC_nH_m, $Ni_kC_nH_m$, and $Ni_k(C_6H_6)_2$ where $k \leq 4$ and $m \leq n \leq$

(23) S. Prigge and E. Bauer, "Springer Series in Chemical Physics", Vol. 9, A Benninghoven et al., Eds., Springer-Verlag, Berlin, 1979, p 133.
(24) N. Winograd, B. J. Garrison, and D. E. Harrison, Jr., *Phys. Rev. Lett.*, **41**, 1120 (1978).
(25) S. P. Holland, B. J. Garrison, and N. Winograd, *Phys. Rev. Lett.*, **43**, 220 (1979).
(26) S. P. Holland, B. J. Garrison, and N. Winograd, *Phys. Rev. Lett.*, **44**, 756 (1980).
(27) S. Kapur and B. J. Garrison, *J. Chem. Phys.*, **75**, 445 (1981); *Surf. Sci.*, **109**, 435 (1981).
(28) R. A. Gibbs, S. P. Holland, K. E. Foley, B. J. Garrison, and N. Winograd, *Phys. Rev. B*, **24**, 6178 (1981).

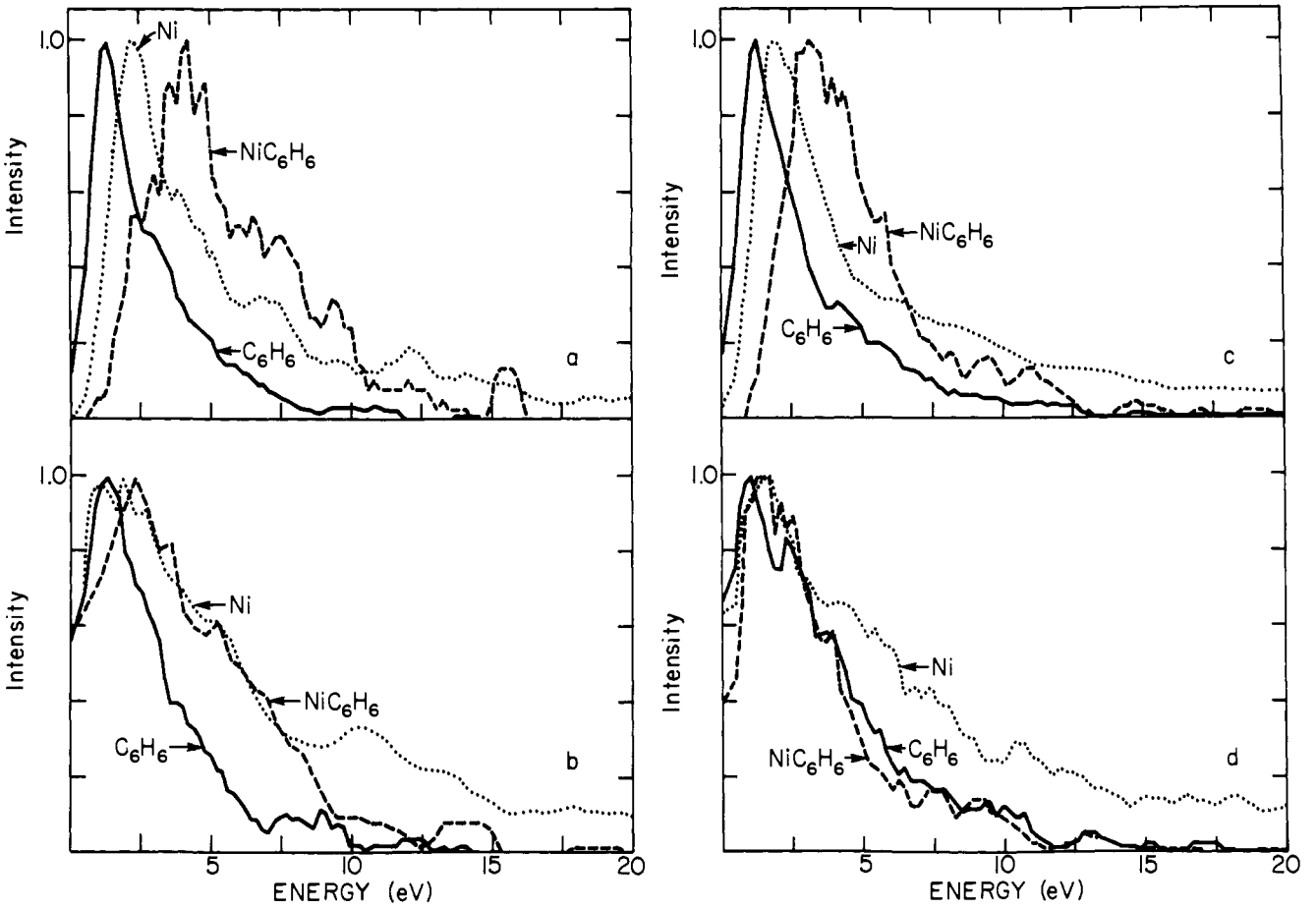

Figure 7. Energy distributions: (a) uncorrected distributions from the SIMS simulation; (b) distributions from the SIMS simulation corrected for a 1.8-eV image force;[9,18,28] (c) uncorrected distributions from the PDMS simulation; (d) distributions from the PDMS simulation corrected for a 1.8-eV image force.[9,18,28]

6. A preliminary analysis of the internal vibrational energy of the benzene molecules indicates that ~75% of them have less than 5 eV of energy, thus we would not expect there to be a significant amount of fragmentation on the way to the detector. The experimental SIMS spectrum for the system of a $c(4 \times 4)$ overlayer of benzene molecules on Ni(001) is also dominated by the parent species in the form of a cationized cluster, $NiC_6H_6^+$.[29]

The calculated energy distributions of the Ni atoms, C_6H_6 molecules, and NiC_6H_6 clusters are very similar to those from the SIMS calculation (Figure 7a,c). In both cases the Ni and C_6H_6 distributions peak at lower energies than the NiC_6H_6 distribution. The calculated distributions are corrected for the influence of the negative charge polarization in the metal as the ion leaves the surface[9,28] to obtain energy distributions that are comparable to the experimental ones of the ejecting Ni^+ and $NiC_6H_6^+$ ions. Energy must be expended to overcome this image force. The corrected Ni and C_6H_6 distributions now peak at about the same energy (Figure 7b,d). This is in agreement with recent SIMS experiments of the C_6H_6/Ni(001) system by Karwacki and Winograd.[29]

It is interesting to note that although the Ni atom distributions from both the SIMS and PDMS calculations have high-energy tails, the C_6H_6 distributions are almost Maxwell–Boltzmann-like in form. However, both the Ni and C_6H_6 distributions arise from the same collision cascade. Thus it is not straightforward to use energy distributions as a definitive guide to the type of processes that may be important for the desorption. The Maxwell–Boltzmann-like distribution in this case did not arise from a thermal equilibrium but rather from an energetic collision cascade process where the high-energy particles have been selectively deleted.

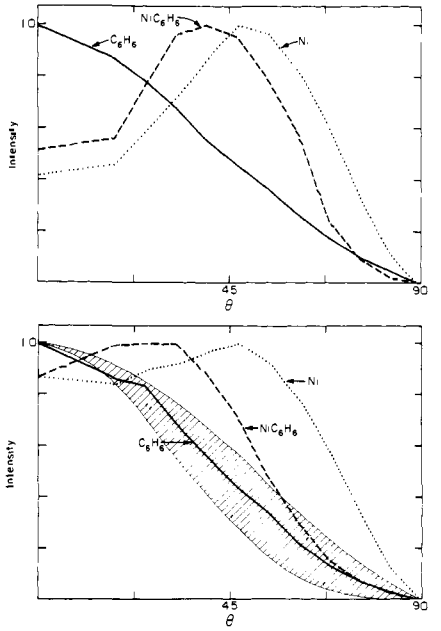

Figure 8. Polar angle distributions. The azimuthal angle of collection is along the ⟨100⟩ direction. The polar resolution is ±12.5°. The top panel is from the SIMS simulation and the bottom from the PDMS simulation. The shaded area is bracketed by lines of $\cos^{1.5}\theta$ and $\cos^{3.5}\theta$. Only particles with less than 20 eV of kinetic energy are collected.

Energy distributions of molecular species ejected during SIMS experiments[30] as well as PDMS experiments[5] are in qualitative

(29) E. J. Karwacki and N. Winograd, *Anal. Chem.*, in press.

(30) D. W. Moon and N. Winograd, to be published.

agreement with the calculated C_6H_6 distribution.

The polar angle distribution of C_6H_6 molecules ejected in the PDMS calculation is similar to that from the SIMS simulation (Figure 8). Both are peaked at normal ejection ($\theta = 0°$). Experimental PDMS distributions of atomic species have been fit to the $\cos^n \theta$ form where $n \approx 2.5 \pm 1$.[10] The distributions in Figure 8 follow this same general behavior, especially the C_6H_6 distribution. It is difficult, however, to uniquely determine the exponent n since the curvature of the distribution depends on the polar angle resolution of the collection scheme. The Ni polar distribution reflects the enhanced, relative to the SIMS results, normal ejection due to the forward scattering process. The peak at $\theta = 45°$ is partly due to the single-crystal nature of the substrate. As a result this curve does not follow the $\cos^n \theta$ relationship quite as well as the benzene distribution. As in the SIMS case the NiC_6H_6 clusters form from a rearrangement process of ejecting Ni atoms and C_6H_6 molecules,[18] thus their polar distribution reflects to a large degree the Ni-atom distribution. Inclusion of the image force correction results in the peak of the Ni and NiC_6H_6 distributions occurring at a larger angle. The C_6H_6 distribution, however, is not significantly altered.

Conclusions

The classical dynamics procedure has been used to model the desorption of atoms and organic molecules from surfaces due to heavy particle bombardment from the backside of the sample. For the desorption of organic molecules the predicted mass spectrum is similar to that obtained from calculations where the incident particle bombards from the frontside. The energy distribution of the C_6H_6 molecules from both calculations is Maxwell–Boltzmann-like, in agreement with the experiment, even though a thermal equilibrium is not established. The PDMS Ni energy distributions, however, exhibit a higher energy tail than those from the SIMS simulation. The azimuthal angular distributions of the Ni atoms are distinctly different from the two calculations.

We find collisional mechanisms which are important for the desorption process in this PDMS simulation which are not important in SIMS simulations. Most of the differences can be traced to conservation of linear momentum. We believe that because of the differences in the important collision mechanisms for desorption it may be possible for larger molecules to be desorbed in the PDMS experiments than in SIMS or FABMS experiments. If a molecule is bonded to a substrate at several places, desorption may require a simultaneous (within $\sim 10^{-14}$–10^{-13} s) severing of most of the bonds. It is more difficult to obtain coherent upward motion of atoms subsequent to frontside bombardment than to obtain this in-phase atomic motion from an energetic particle bombarding from the backside. The calculations presented here also offer a number of experimentally testable predictions, for example, the energy and angular distributions of monoelemental single crystals, which should help to conclusively elucidate the important desorption mechanism using PDMS.

Acknowledgment. We wish to thank the National Science Foundation (Grant No. CHE-8022524) and the Office of Naval Research for financial support as well as acknowledge the A. P. Sloan Foundation for a Research Fellowship and the Camille and Henry Dreyfus Foundation for a grant for newly appointed young faculty. We thank R. D. Macfarlane and C. J. McNeal for spirited and helpful discussions.

Registry No. Ni, 7440-02-0; C_6H_6, 71-43-2.

Nature of π-Electron-Transfer Effects in Organic Systems with Varying π-Electron Demand

William F. Reynolds,*[1a] Photis Dais,[1a] Douglas W. MacIntyre,[1a] Ronald D. Topsom,*[1b] Stephen Marriott,[1b] Ellak von Nagy-Felsobuki,[1b] and Robert W. Taft*[1c]

Contribution from the Department of Chemistry, University of Toronto, Toronto, Canada M5S 1A1, Department of Organic Chemistry, La Trobe University, Bundoora, Australia 3083, and Department of Chemistry, University of California, Irvine, Irvine, California 92717. *Received May 6, 1982*

Abstract: Calculations using an ab initio molecular orbital basis (STO-3G or 4-31G) for a series of substituted probe molecules covering a wide range of π-electron demand have revealed a complex pattern of substituent resonance response to varying electron demand. The results support the suggested amphielectronic behavior of π-acceptor substituents such as CF_3, CHO, CN, and NO_2. In spite of these complexities, the resonance response patterns of individual substituents attached to aromatic molecules can be reasonably approximated by certain bilinear relationships. Comparison of calculations with experimental data for gas-phase pyridinium ion and phenol acidities offers confirmation of the recently defined $\sigma_R^+{}_{(g)}$ and $\sigma_R^-{}_{(g)}$ scales. For π-acceptor substituents (+R) in electron-rich systems, the $\sigma_R^-{}_{(g)}$ scale is shown to extend all the way to XCH_2^-, i.e., for the gas-phase acidities of substituted methanes. Evidence is provided for leveling effects of strong π-donor substituents (-R) under strong electron demand, e.g., for both XCH_2^+ cations and XCH_2^- anions.

It has long been recognized that the electronic effect of a substituent depends to a certain extent upon the electron demand in the system to which it is attached. In the context of the Hammett equation, this has been handled by defining different σ constant scales for systems with different electron demand (e.g., σ, σ^0, σ^+, σ^-, etc.).[2]

An alternative approach to substituent effects is to divide the total electronic effect of a substituent into field/inductive and resonance contributions, that is, to use a dual substituent parameter

(1) (a) University of Toronto. (b) La Trobe University. (c) University of California, Irvine. This work was supported in part by grants from the National Science Foundation (UCI) and the Australian Research Grants Scheme (La Trobe).

(2) (a) Hammett, L. P. "Physical Organic Chemistry"; McGraw-Hill: New York, 1940. (b) Hine, J. "Structural Effects In Equilibria in Organic Chemistry"; Wiley-Interscience: New York, 1975; Chapter 3.

0002-7863/83/1505-0378$01.50/0